High-Frequency Reciprocity Based Circuit Model for the Incidence of Electromagnetic Waves on General Circuits in Layered Media

Frank Olyslager, *Member, IEEE*

Abstract— **Traditionally a circuit on a high-speed multichip module (MM) or a microwave monolithic integrated circuit (MMIC) is represented in an equivalent circuit by S-parameters for the different components, such as filters or bends, and by transmission lines for the interconnections between the components. Nowadays the S-parameters of the components are easily determined by a numerical electromagnetic analysis. Different components close to each other will interact, often this interaction is unwanted. In the present contribution we develop a circuit model for these interactions without having to perform a global electromagnetic analysis of the interacting components. These interactions are then represented by discrete and distributed sources in the equivalent circuit. Our technique is based on reciprocity and is focused on the surface wave interaction which is often the most important one. Each component is characterized by a surface wave radiation pattern.**

I. Introduction

MULTICHIP modules (MCM's) and microwave monolithic integrated circuits (MMIC's) typically consist of metalization patterns embedded in a layered structure. Certainly for a MCM, and often also for a MMIC, it is not possible to perform a global electromagnetic simulation that incorporates all the interactions between the different circuits on a MCM or MMIC. Modeling large parts of a circuit at once is very CPU-time consuming and often impractical because every time the design of the circuit is changed the modeling has to be repeated. Due to the layered nature of the substrate the most important interaction between different separated circuits on the same MCM or MMIC is surface wave coupling. Our aim is to characterize each circuit by a surface wave radiation pattern and to represent the interaction of a surface wave with a circuit by a current and voltage source in the circuit model of the circuit. In essence we approach the problem as a transmitter and receiver surface wave antenna problem.

A typical circuit on a MCM or MMIC consists of interconnections and what we will call components. These components are everything which deviates from an interconnection structure such as bends, steps in width, filters, active components, lumped elements, via holes, air bridges, etc.. In a high frequency circuit description the interconnections, which act as waveguides, are represented by an equivalent transmission line model and the components are represented by their S-parameters. In the past much theoretical effort has been spent in constructing equivalent transmission line models for high-frequency interconnections. In [1] a rigorous equivalent transmission line model has been derived based on reciprocity considerations. In the same publication the meaning of the impedance level of the transmission line model and at the same time the meaning of S-parameters for connected components has been carefully investigated. In [2], based on the same equivalent transmission line model and on the Lorentz reciprocity relation, a circuit model for the incidence of electromagnetic waves on interconnections has been investigated. The impinging wave is represented as distributed current and voltage sources in the transmission line. Traditionally, components are described by their S-parameters at the ports where the electromagnetic field is assumed to be modal. Nowadays electromagnetic field simulators are available to determine the S-parameters of a very large variety of components.

Although we will mainly concentrate on surface wave coupling, it will be shown that other coupling mechanisms such as space wave coupling can be handled with the same techniques. Because of their importance and to make the theory more intelligible we will start with planar perfectly conducting circuits. Later the generalization to general three dimensional, not necessary perfectly conducting, objects embedded in layered media will be discussed. This makes the theory also applicable to dielectric waveguide circuits.

II. Schematic Representation

To focus our attention let us consider the planar metalization structure of Fig. 1. The figure shows the top view of the structure and it is assumed that the metalization is located inside or on top of a stack of layers which can be backed with a ground plane. The structure consists of two separated circuits, indicated with A and B. Each circuit consists of a number (two in the case of the figure) of interconnections (hatched regions on the figure) and a component part. The interconnections, indicated by the subscripts '$I,1$', '$I,2$', etc., provide interaction with the external world, i.e., with other circuits. In the sequel we will assume two interconnections for each component but the theory is of course valid for any number of interconnections. The component part, indicated by the subscript 'C' is an irregular planar metalization pattern,

Manuscript received June 12, 1995; revised February 15, 1996

The author is with the Department of Information Technology, University of Ghent, 9000 Ghent, Belgium.

Publisher Item Identifier S 0018-9480(96)03803-3.

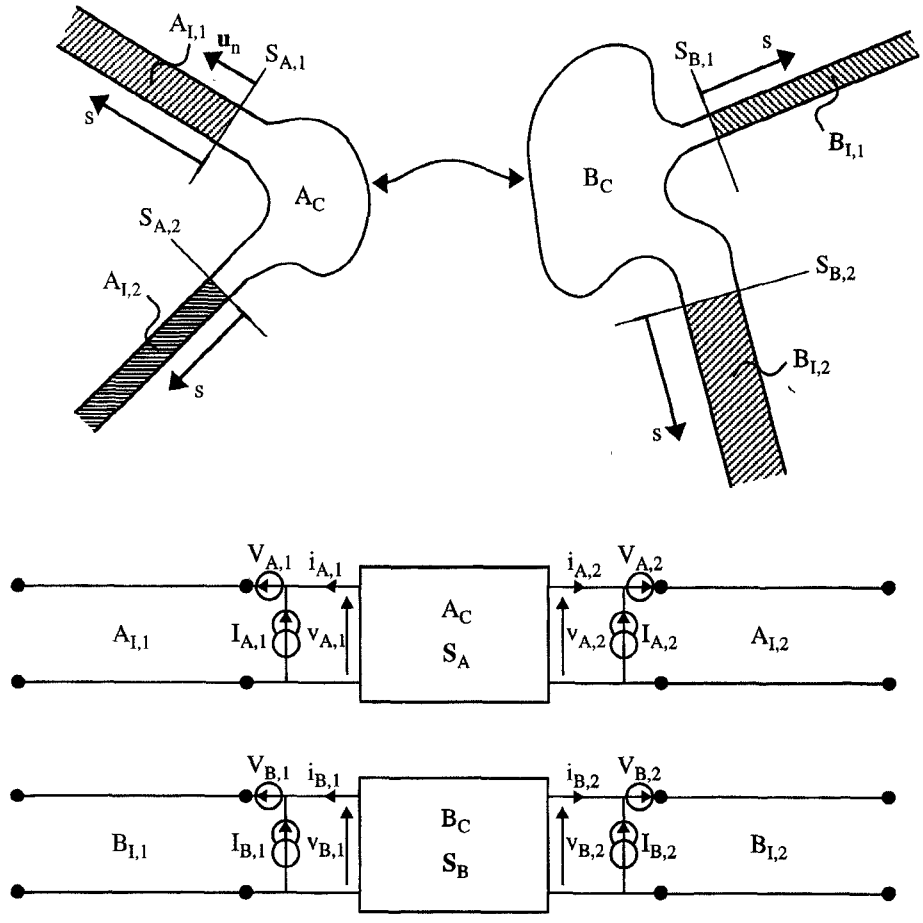

Fig. 1. Interaction between the component parts of two planar metalization structures and the corresponding representation by discrete sources.

such as a filter, a step in width or just a bend. The places where the interconnections are connected to the component part are called the ports of the component.

Suppose for a moment that only circuit A is present and that we have modeled this structure with an electromagnetic simulator. From this simulation we know the current densities on the metalization for each excitation of the structure by a fundamental mode on the interconnections $A_{I,1}$ and $A_{I,2}$. It is assumed that the fields along the interconnection parts $A_{I,1}$ and $A_{I,2}$ are monomodal and that other higher order modes, discrete or continuous, generated in the component part A_C have died out and are negligible compared to the fundamental modes at the ports. If this is not the case then the interconnection part must be reduced and the component part must be enlarged. From the electromagnetic simulation we obtain a circuit model for circuit A consisting of two transmission lines, which represent the interconnections, and a scattering parameter matrix $\boldsymbol{S}_A$ which describes the component part A_C. It has to be remarked that if the interconnection propagates more than one fundamental mode (for example an even and odd mode in two parallel microstrips) or if also higher order modes are important, for example at higher frequencies, the interconnections can be represented by a coupled set of transmission lines. The generalization of the theory to multimode interconnections is presented in Appendix A. A similar electromagnetic simulation for the circuit B yields the surface current densities on the metalization and the scattering parameter matrix S_B.

If both circuits are present they will interact. This means that the whole structure starts to act as a four-port. One way to characterize this structure is to perform one global electromagnetic simulation for the whole structure and derive the 4×4 scattering parameter matrix of the structure. This might still be manageable for the simple structure depicted in Fig. 1 but this technique is certainly to CPU-time consuming for a whole MCM. To overcome this problem we will adopt a different technique to take into account the interaction between circuit A and B. However, we have to make the assumption that the effect of the presence of circuit B on circuit A is negligible when circuit B is not excited at its interconnections. Clearly this assumption will fail, e.g., if circuit A and B are parts of the same filter structure which is designed to have strong interaction between its different parts. However, when circuit A and B are truly two different structures then the present method will be able to calculate the electromagnetic interference between both circuits. For planar structures in layered media the most important interaction between such different structures is due to surface waves. These surface waves are eigenmodes of the layered structure in the absence of the metalization patterns and they are excited by the current densities on discontinuities, such as the components A_C and B_C. Except for this surface wave interaction, there is also

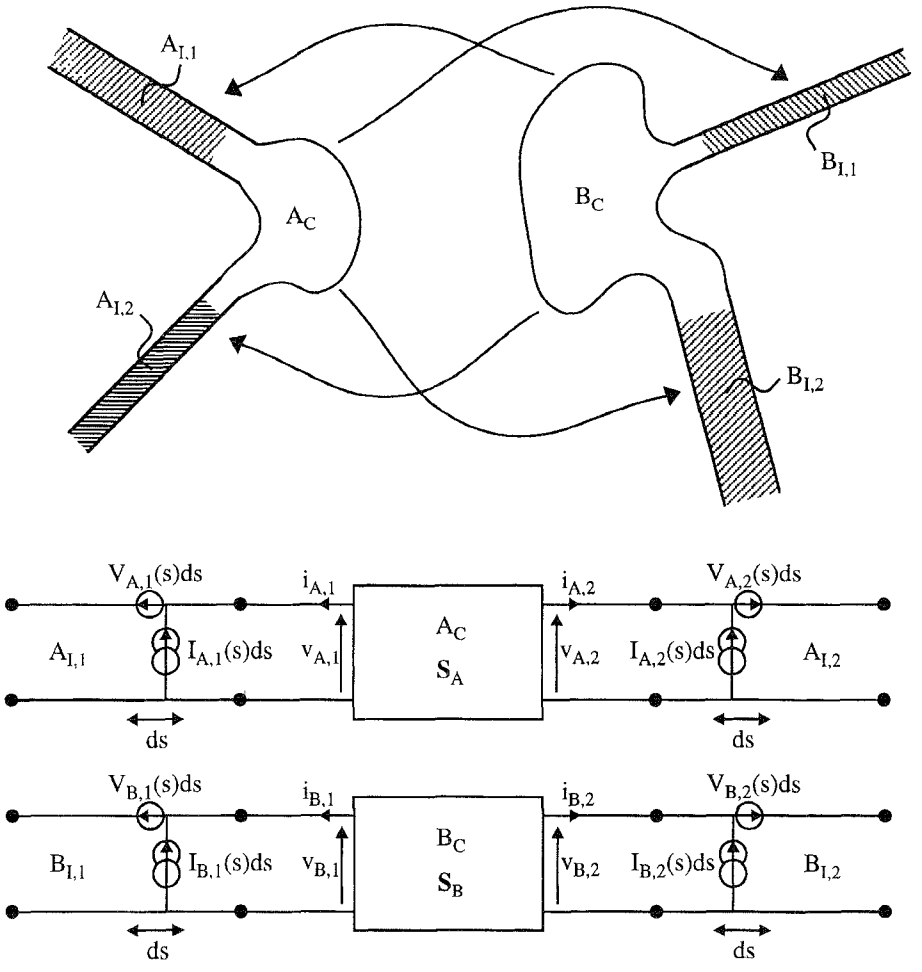

Fig. 2. Interaction between the fields generated at the component parts with the interconnection parts of the other structure and representation by distributed sources.

interaction through space waves, i.e., through radiation in the air above the metalization. In this case A_C and B_C act as real antennas. However, it is often the surface wave interaction which is dominant because the surface waves decay more slowly than the space waves as a function of the radial distance.

Now we will give a schematic overview and circuit representation of the interaction between circuits A and B. We will separate the interaction between structure A and B into four parts. The first type of interaction together with the circuit model is shown in Fig. 1. This first type of interaction takes into account the incidence of electromagnetic waves, generated by the currents of A_C, on B_C and vice versa. So if circuit A is excited by a mode along one of its interconnections, the currents on A_C will generate surface waves. These surface waves will induce currents on B_C and excite the fundamental eigenmodes, which propagate away from B_C, in the interconnections $B_{I,1}$ and $B_{I,2}$. In the circuit model this interaction is represented by the current and voltage sources $I_{B,1}, I_{B,2}, V_{B,1}$, and $V_{B,2}$ at the ports of structure B which depend on the currents and voltages $i_{A,1}, i_{A,2}, v_{A,1}$, and $v_{A,2}$ at the ports of circuit A. Indeed $i_{A,1}, i_{A\,2}, v_{A,1}$ and $v_{A,2}$ determine or represent by what amount the eigenmodes in the interconnections of structure A are excited and $I_{B,1}, I_{B,2}, V_{B,1}$, and $V_{B,2}$ represent the excitation of the eigenmodes in the ports of structure B. The sources $I_{B,1}$ and $V_{B,1}(I_{B,2}$ and $V_{B,2})$ are designed such that they generate a wave or mode in the transmission line $B_{I,1}(B_{I,2})$ which propagates away from the component B_C. Due to linearity the sources $I_{B,1}, I_{B,2}, V_{B\,1}$, and $V_{B,2}$ are linear combinations of the circuit parameters $i_{A,1}, i_{A,2}, v_{A,1}$, and $v_{A,2}$. The above reasoning can be repeated when surface waves generated in B_C interact with A_C.

Fig. 2 depicts the second type of interaction. The surface waves generated at A_C will not only generate eigenmodes in the interconnections $B_{I,1}$ and $B_{I,2}$ through interaction with the component part B_C of circuit B but also directly through interaction with the interconnections $B_{I,1}$ and $B_{I,2}$ themselves. The interaction of impinging waves on interconnections was studied in detail in [2]. The circuit equivalent of this type of interaction is also shown in Fig. 2. The interaction is represented by distributed sources $I_{B,1}(s)\ ds, I_{B,2}(s)\ ds, V_{B,1}(s)\ ds$, and $V_{B,2}(s)\ ds$ in the transmission lines which depend on the currents and voltages $i_{A,1}, i_{A,2}, v_{A,1}$, and $v_{A,2}$ at the ports of A_C. Here s denotes the distance from the component along the considered transmission line. Of course by a simple integration it is possible to concentrate the distributed sources along a part of a transmission line in a discrete source placed at some

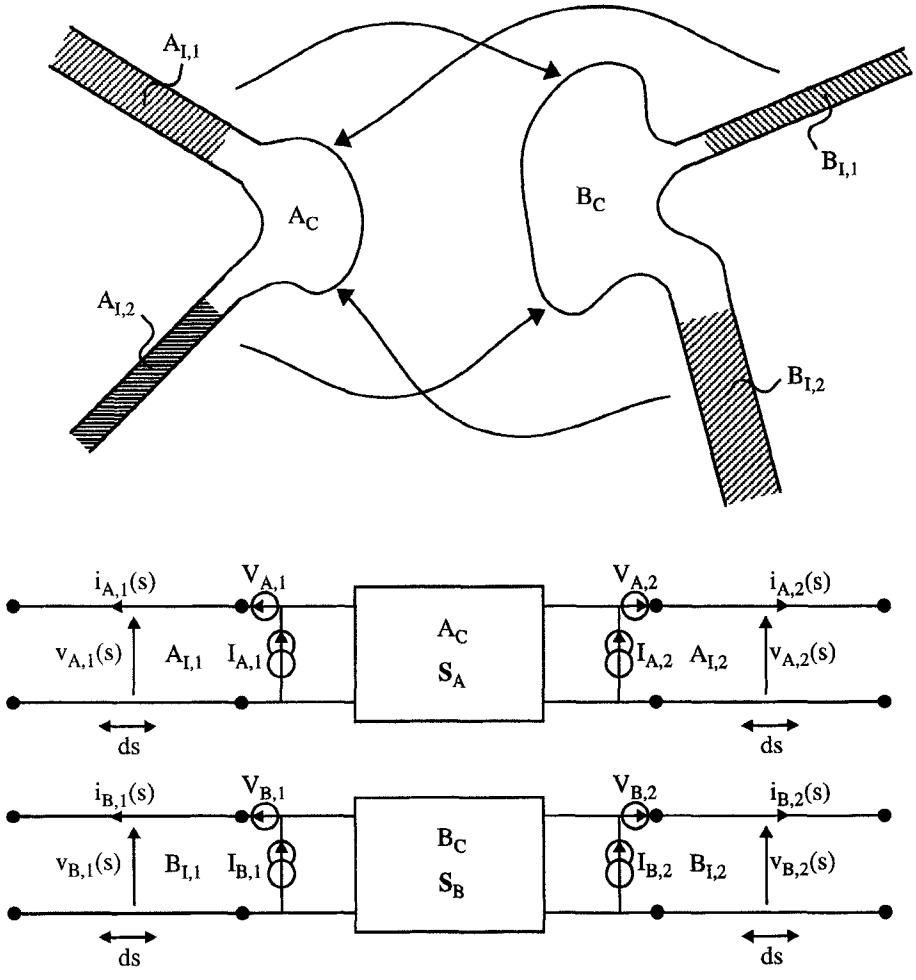

Fig. 3. Interaction between the fields generated at the interconnection parts with the component part of the other structure and representation by discrete sources.

point of that part. This discrete source will have the same effect outside the considered part of the transmission line as the distributed sources on that part.

Normally an eigenmode propagating along an infinite interconnection or waveguide does not interact with surface waves. This is however not true for a finite or semi-infinite interconnection line. This brings us to a third type of interaction which is the reciprocal of the previous type. The interconnections $A_{I,1}$ and $A_{I,2}$ will generate surface waves which, through interaction with B_C will generate eigenmodes in the interconnections $B_{I,1}$ and $B_{I,2}$. This situation is shown in Fig. 3 together with the circuit equivalent. The circuit equivalent consists of discrete sources $I_{B,1}, I_{B,2}, V_{B,1}$, and $V_{B,2}$ at the ports of B_C which depend on the currents and voltages $i_{A,1}(s), i_{A,2}(s), v_{A,1}(s)$, and $v_{A,2}(s)$ of each elementary part ds of the interconnections $A_{I,1}$ and $A_{I,2}$. Of course one could again integrate along a part of the interconnections $A_{I,1}$ or $A_{I,2}$ to concentrate the effect of this part into one contribution. As mentioned, this third type of interaction is reciprocal to the second type of interaction. This allows us to draw an interesting conclusion. Since an eigenmode on an infinite interconnection does not generate surface waves it is to be expected that for a semi-infinite interconnection only the part near the end, i.e., near the port of the interconnection, will generate substantial surface waves. The contribution from parts further away from the port will be less important. Each part of the semi-infinite transmission line will generate the same amount of surface waves but for the parts further away from the port there will be a more and more destructive interference between the surface waves generated by different parts. This means that we can restrict ourselves to the contribution of a small part of $A_{I,1}$ and $A_{I,2}$ close to A_C. And from reciprocity this means that for the second type of interaction we can restrict ourselves to the contribution of distributed sources close to A_C or B_C.

From the third type of interaction it is natural to deduce the fourth type of interaction. The surface waves generated by the interconnections $A_{I,1}$ and $A_{I,2}$ will also directly generate eigenmodes in the interconnections $B_{I,1}$ and $B_{I,2}$. The circuit model for this type of interaction consists of distributed sources $I_{B,1}(s)\ ds, I_{B,2}(s)\ ds, V_{B,1}(s)\ ds$, and $V_{B,2}(s)\ ds$ in the transmission lines which depend on the currents and voltages $i_{A,1}(s), i_{A,2}(s), v_{B,1}(s)$, and $v_{B,2}(s)$ in each elementary part ds of the interconnections $A_{I,1}$ and $A_{I,2}$.

Due to the fact that interconnections do not interact very strongly with surface waves, it is clear that the first type of interaction is the most important one and the fourth type of interaction is the least important one. In this paper we will concentrate on this first type. In essence the third type of interaction is only a special case of the first type which

means that with the theory of this paper it is also possible to calculate this interaction. The second and also the fourth type of interaction can be calculated with the theory of [2].

III. The Excitation or Transmitter Problem

In this section we determine the surface waves (and also space waves) generated by the component part A_C when the voltages and currents $v_{A,1}, v_{A,2}, i_{A,1}$, and $i_{A,2}$ in the circuit model at the ports, i.e., at $s = 0$, are known (Fig. 1). We assume that the circuit model for the structure A was based on the reciprocity definition introduced in [2]. First of all we observe that $v_{A,1}, v_{A,2}, i_{A,1}$, and $i_{A,2}$ are not fully independent, they are related through the $\boldsymbol{S}_A$-matrix.

The voltage and current on both transmission lines can be written as two waves or modes, one propagating in the positive direction and one in the negative direction

$$\begin{aligned} v_{A,i}(s) &= 2(I_{m,A,i})^{-1}\exp(-j\beta_{A,i}s)K^{+}_{A,i} \\ &\quad + 2(I_{m,A,i})^{-1}\exp(j\beta_{A,i}s)K^{-}_{A,i} \\ i_{A,i}(s) &= I_{m,A,i}\exp(-j\beta_{A,i}s)K^{+}_{A,i} \\ &\quad - I_{m,A,i}\exp(j\beta_{A,i}s)K^{-}_{A,i} \end{aligned} \tag{1}$$

with $i = 1, 2$ and where $\beta_{A,i}$ is the propagation coefficient of the fundamental mode on interconnection line $A_{I,i}$. $K^{+}_{A,i}$ and $K^{-}_{A,i}$ are the excitation coefficients of the normalized fundamental mode propagating in the positive and negative direction, respectively. $I_{m,A,i}$ is the total longitudinal current of the normalized fundamental mode. Note that the characteristic impedance $Z_{\mathrm{char},A,i}$ is given by $2(I_{m,A,i})^{-2}$. The model (1) is a reciprocity-current (RI) based transmission line model [1] for the interconnections. If $\boldsymbol{E}_{\mathrm{tr},A,i}$ and $\boldsymbol{H}_{\mathrm{tr},A,i}$ are the transversal field components of the fundamental mode then this mode is normalized if

$$\frac{1}{2}\iint_{S_{-A,i}} (\boldsymbol{E}_{\mathrm{tr}A,i} \times \boldsymbol{H}_{\mathrm{tr},A,i}) \cdot \boldsymbol{u}_n \, dS = 1 \tag{2}$$

where u_n is the unit vector along the line perpendicular to the transverse plane $S_{A,i}$.

Using (1) it is possible to determine the excitation coefficients $K^{+}_{A,i}$ and $K^{-}_{A,i}$ if $v_{A,i}$ and $i_{A,i}$ at $s = 0$ are known by simply inverting (1) for $s = 0$. The result is

$$K^{\pm}_{A,i} = \tfrac{1}{4}\left[I_{m,A,i}v_{A,i}(s=0) \pm 2(I_{m,A,i})^{-1}i_{A,i}(s=0)\right]. \tag{3}$$

This is the first step in the excitation problem. Given $v_{A,i}$ and $i_{A,i}$ at $s = 0$ we are able to determine by what amount the eigenmodes in the lines are excited.

If the structure A is excited by a normalized mode along for example $A_{I,1}$ then we get the following current densities on the structure A

$$\begin{aligned} \boldsymbol{J}^{(1)}_{A,1} &= \exp(j\beta_{A,1}s)(-J_{s,A,1}\boldsymbol{u}_s + J_{\mathrm{tr},A,1}\boldsymbol{u}_{\mathrm{tr}}) \\ &\quad + S_{A,11}\exp(-j\beta_{A,1}s)(J_{s,A,1}\boldsymbol{u}_s + J_{\mathrm{tr},A,1}\boldsymbol{u}_{\mathrm{tr}}) \\ &\qquad\qquad \text{on } A_{I,1} \\ \boldsymbol{J}^{(1)}_{A,2} &= S_{A,12}\exp(j\beta_{A,2}s)(J_{s,A,2}\boldsymbol{u}_s + J_{\mathrm{tr},A,2}\boldsymbol{u}_{\mathrm{tr}}) \quad \text{on } A_{I,2} \\ \boldsymbol{J}^{(1)}_{A} &\qquad\qquad \text{on } A_C \end{aligned} \tag{4}$$

where $J_{s,A,i}$ and $J_{\mathrm{tr},A,i}$ are the current densities of the normalized mode on interconnection $A_{I,1}$ in the longitudinal and transversal direction, respectively. $\boldsymbol{S}_{A,ij}$ are the elements of the scattering matrix $\boldsymbol{S}_A$ defined in [2]. The current density $\boldsymbol{J}^{(1)}_A$ follows from an electromagnetic simulation of the structure A. Similar current densities ($\boldsymbol{J}^{(2)}_{A,1}, \boldsymbol{J}^{(2)}_{A,2}$, and $\boldsymbol{J}^{(2)}_A$) as in (4) are generated when a mode is incident along $A_{I,2}$.

We are now interested in the fields generated by the current densities $\boldsymbol{J}^{(i)}_A, i = 1, 2$ and especially in the generated surface waves. It is possible to calculate these fields using different approaches. Since we consider planar metalizations it is suitable to use a mixed-potential formulation [3]

$$\begin{aligned} \boldsymbol{E}^{(i)}_t(\boldsymbol{r}) &= \iint_{A_C} [G_{A,tt}(\boldsymbol{r},\boldsymbol{r}')\boldsymbol{J}^{(i)}_A(\boldsymbol{r}') \\ &\quad - \nabla_t G_\phi(\boldsymbol{r},\boldsymbol{r}')\nabla'_t \\ &\quad \cdot \boldsymbol{J}^{(i)}_A\boldsymbol{r}')] \, dS' \\ &= \iint_{A_C} \{[G_{A,tt}(\boldsymbol{r},\boldsymbol{r}')\boldsymbol{I}_{tt} \\ &\quad - \nabla_t\nabla_t G_\phi(\boldsymbol{r},\boldsymbol{r}')] \\ &\quad \cdot \boldsymbol{J}^{(i)}_A(\boldsymbol{r}')\} \, dS'. \end{aligned} \tag{5}$$

The subscript 't' denotes quantities parallel to the xy-plane. We restricted ourselves to the xy-components of the electric field because we will only need these components in the sequel. $G_{A,tt}$ and G_ϕ are scalar magnetic and electric Green's functions, $\boldsymbol{I}_{tt}$ is the two-dimensional (2-D) unit dyadic in the xy-plane and $\nabla_t\nabla_t$ is a dyad. Since these Green's functions only depend on z, z' and the radial distance ρ between $\boldsymbol{r}$ and $\boldsymbol{r}'$, i.e., $\rho = |\boldsymbol{u}_z \times (\boldsymbol{r} - \boldsymbol{r}')|$, we write them as $G_{A,tt}(\rho, z|z')$ and $G_\phi(r, z|z')$. Due to the layered nature of the structure these Green's functions are first determined analytically in the spectral domain and are then numerically inverse Fourier transformed

$$G(\rho, z|z') = \frac{1}{2\pi}\int_0^{+\infty} G(\lambda, z|z')J_0(\lambda\rho)\lambda \, d\lambda \tag{6}$$

where $G(\rho, z|z')(G(\lambda, z|z'))$ is $G_A(\rho, z|z')(G_A(\lambda, z|z'))$ or $G_\phi(\rho, z|z')(G_\phi(\lambda, z|z'))$ and where λ is the radial spectral variable. Using Cauchy's residue theorem and after some algebra we can rewrite (6) as [4], [5]

$$\begin{aligned} G(\rho, z|z') &= \frac{1}{4\pi}\int_{-j\infty}^{j\infty} G(\sqrt{\Gamma^2 + k_u^2}, z|z') \\ &\quad \cdot H^{(2)}_0(\sqrt{\Gamma^2 + k_u^2}\rho)\Gamma \, d\Gamma \\ &\quad - \frac{j}{2}\sum_\nu G_\nu(z|z')H^{(2)}_0(\lambda_\nu\rho)\lambda_\nu. \end{aligned} \tag{7}$$

The first term is the contribution from a branch cut, i.e., the first term represents the space wave contribution. In (7) we assumed that there was a semi-infinite layer at the top of the structure and a metal plane at the bottom. If there is also a semi-infinite layer at the bottom of the structure an extra branch-cut integral has to be introduced. In (7) the wavenumber k_u is given by $\omega\sqrt{\epsilon_u\mu_u}$ with ϵ_u and μ_u the material parameters of the semi-infinite layer. The square roots

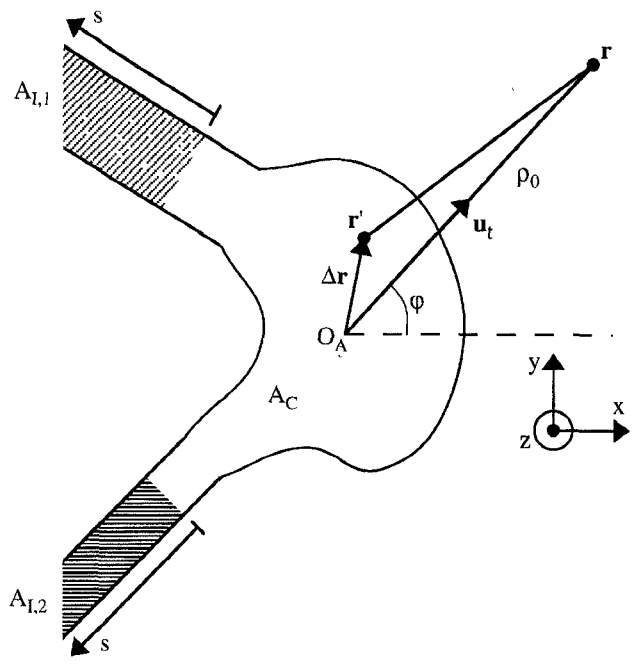

Fig. 4. Notations for the far field contribution of the surface waves generated by the component part A_C of structure A.

in the integrand of (7) are defined such that their imaginary part is not positive. $H_0^{(2)}$ is the Hankel function of second kind and order zero with its branch-cut along the negative real axis. The second term in (7) represents the surface wave contributions. The quantities λ_ν ($\mathrm{Im}(\lambda_\nu) \leq 0$) are the propagation coefficients of these surface waves, i.e., of the eigenmodes of the multilayered slab waveguide structure, and $G_\nu(z|z')$ is the residue of $G(\lambda, z|z')$ at $\lambda = \lambda_\nu$

$$G_\nu(z|z') = \lim_{\lambda \to \lambda_\nu} [G(\lambda, z|z')(\lambda - \lambda_\nu)]. \tag{8}$$

Since the amplitude of the surface waves only decays as $1/\sqrt{\rho}$ and that of the space waves as $1/r$, the surface waves become dominant after some distance. This means that after some distance from A_C the main contribution in (5) comes from the surface waves. The contribution from surface wave ν is given by

$$\boldsymbol{E}_{t,\nu}^{(i)}(\boldsymbol{r}) = -\frac{j}{2}\lambda_\nu \iint_{A_C} [G_{A,tt,\nu}(z,z')H_0^{(2)}(\lambda_\nu\rho)\boldsymbol{J}_A^{(i)}(\boldsymbol{r}') - \nabla_t\nabla_t G_{\phi,\nu}(z,z')H_0^{(2)}(\lambda_\nu\rho)\cdot\boldsymbol{J}_A^{(i)}(\boldsymbol{r}')]\, dS'. \tag{9}$$

In a last step we look at the far field contribution of a surface wave. If we insert the asymptotic form of the Hankel function [6] in (9) and use the notations of Fig. 4 we obtain

$$\boldsymbol{E}_\nu^{(i)}(\boldsymbol{r}) \approx -\frac{(j-1)}{2}\sqrt{\frac{\lambda_\nu}{\pi\rho_0}}\exp(-j\lambda_\nu\rho_0) \cdot \{G_{A,tt,\nu}(z|z')\boldsymbol{f}_\nu^{(i)}(\varphi) + \lambda_\nu^2 G_{\phi,\nu}(z|z')[\boldsymbol{u}_t\cdot\boldsymbol{f}_\nu^{(i)}(\varphi)]\boldsymbol{u}_t\} \tag{10}$$

with

$$\boldsymbol{f}_\nu^{(i)}(\varphi) = \iint_{A_C} \exp(j\lambda_\nu\boldsymbol{u}_t\cdot\Delta\boldsymbol{r})\boldsymbol{J}_A^{(i)}(\boldsymbol{r}')\, dS' \tag{11}$$

where the unit vector $\boldsymbol{u}_t$ is in the xy-plane. The functions $\boldsymbol{f}_\nu^{(i)}(\varphi)$ are the surface wave radiation patterns for the part A_C with respect to an arbitrary origin O_A located inside A_C. These functions fully characterize the far field surface wave behavior of A_C.

IV. The Observation or Receiver Problem

Now we want to determine the sources $V_{B,1}, V_{B,2}, I_{B,1}$, and $I_{B,2}$ at the beginning of the transmission lines, i.e., at $s = 0$, generated by a given incident field on the component part B_C. Again a current-reciprocity transmission line model is assumed for the interconnections $B_{I,1}$ and $B_{I,2}$ and the component B_C is characterized through the $\boldsymbol{S}_B$-matrix.

In a first step we determine by what amount the fundamental eigenmodes in the interconnections $B_{I,1}$ and $B_{I,2}$ are excited through the interaction of the incident field $\boldsymbol{E}^{\mathrm{in}}, \boldsymbol{H}^{\mathrm{in}}$ with the component part B_C. This incident field is a field which propagates in the multilayered slab waveguide structure and consists of surface wave and/or space wave contributions. A standard approach to determine the interaction is to invoke the Lorentz reciprocity theorem. To apply this theorem we need to define two fields, labeled 'a' and 'b'. Field 'a' is the scattered field $\boldsymbol{E}^{\mathrm{sc}}, \boldsymbol{H}^{\mathrm{sc}}$ originating from the scattering of the incident field at the metalization of structure B. At the ports of B_C a part of this scattered field will consist of the eigenmodes of the interconnections $B_{I,1}$ and $B_{I,2}$. The transversal components of the modal part of the 'a'-field at these ports are given by

$$\begin{aligned}\boldsymbol{E}_{a,\mathrm{tr}} &= K_{B,i}^+ \exp(-j\beta_{B,i}s)\boldsymbol{E}_{\mathrm{tr},B,i}\\ \boldsymbol{H}_{a,\mathrm{tr}} &= K_{B,i}^+ \exp(-j\beta_{B,i}s)\boldsymbol{H}_{\mathrm{tr},B,i}\end{aligned} \tag{12}$$

where $K_{B,i}^+$ are the yet unknown excitation coefficients of the normalized modes $\boldsymbol{E}_{\mathrm{tr},B,i}, \boldsymbol{H}_{\mathrm{tr},B,i}$ in the interconnections. For the moment we will assume that the modal part (12) of the 'a'-field is far more dominant compared to the remaining scattered part (e.g., surface waves and space waves) at the ports of B_C. The 'b'-field is the field generated in structure B due to an incoming normalized mode along for example the interconnection $B_{I,1}$. Along the interconnection $B_{I,1}$ the transversal field components of this 'b'-field take the following form:

$$\begin{aligned}\boldsymbol{E}_{b,\mathrm{tr}}^{(1)} &= \exp(j\beta_{B,1}s)\boldsymbol{E}_{\mathrm{tr},B,1} + S_{B,11}\exp(-j\beta_{B,1}s)\boldsymbol{E}_{\mathrm{tr},B,1}\\ \boldsymbol{H}_{b,\mathrm{tr}}^{(1)} &= -\exp(j\beta_{B,1}s)\boldsymbol{H}_{\mathrm{tr},B,1} + S_{B,11}\exp(-j\beta_{B,1}s)\boldsymbol{H}_{\mathrm{tr},B,1}\end{aligned} \tag{13}$$

and along the interconnection $B_{I,2}$

$$\begin{aligned}\boldsymbol{E}_{b,\mathrm{tr}}^{(1)} &= S_{B,21}\exp(-j\beta_{B,2}s)\boldsymbol{E}_{\mathrm{tr},B,2}\\ \boldsymbol{H}_{b,\mathrm{tr}}^{(1)} &= S_{B,21}\exp(-j\beta_{B,2}s)\boldsymbol{H}_{\mathrm{tr},B,2}.\end{aligned} \tag{14}$$

In accordance with (4) the corresponding current density on B_C is denoted $\boldsymbol{J}_b = \boldsymbol{J}_B^{(1)}$. Now we apply Lorentz-reciprocity theorem on the volume of which a top-view is shown on Fig. 5. This volume is bounded by the surface Σ which is invariant in the z-direction, i.e., Σ is a cylindrical surface parallel to the z-axis, and which consists partly of the parts of the transverse planes $S_{B,I,1}$ and $S_{B,I,2}$ at the ports where

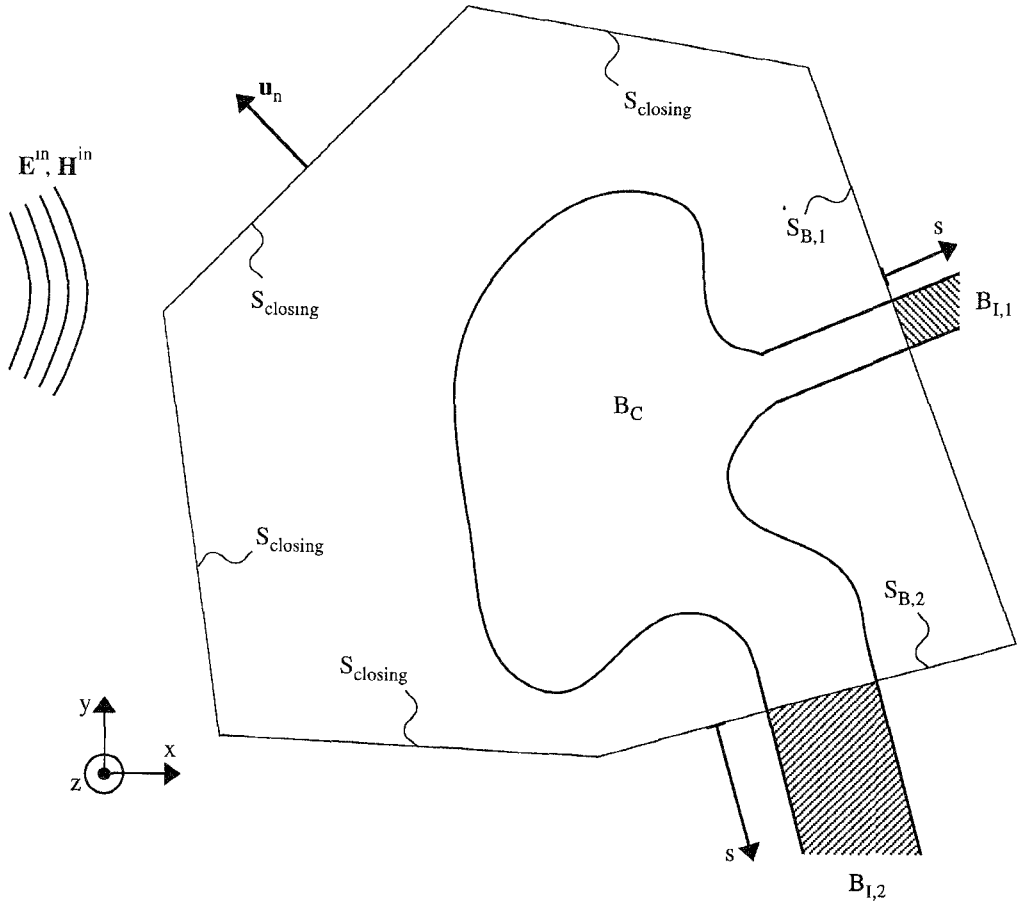

Fig. 5. Cylindrical bounding surface Σ around the structure B_C used for the application of the Lorentz-reciprocity theorem. The surface Σ is composed of S_{closing}, $S_{B,1}$, and $S_{B,2}$.

the modal field patterns are important and partly of a closing surface S_{closing} located far enough from the structure B. In principle this closing surface can be chosen at infinity. The Lorentz reciprocity theorem takes the following form in the defined volume

$$\iint_{\Sigma} (\boldsymbol{E}_a \times \boldsymbol{H}_b - \boldsymbol{E}_b \times \boldsymbol{H}_a) \cdot \boldsymbol{u}_n \, dS = \iint_{B_C} (\boldsymbol{E}_b \cdot \boldsymbol{J}_a - \boldsymbol{E}_a \cdot \boldsymbol{J}_b) \, dS \tag{15}$$

where $\boldsymbol{u}_n$ is the unit vector normal to the surface Σ. If we insert (12), (13) and (14) in (15) and use the fact that $\boldsymbol{E}_b$ is normal to the surface B_C we obtain

$$-4K^{+}_{B,I} = -\iint_{B_C} \boldsymbol{E}^{\text{sc}} \cdot \boldsymbol{J}^{(1)}_B \, dS. \tag{16}$$

It can be shown that the contribution of the closing surface S_{closing} becomes negligibly small when S_{closing} is located far enough from the structure B. Since the tangential component of the total electric field at the surface B_C has to be zero we have that $\boldsymbol{u}_z \times (\boldsymbol{E}^{\text{sc}} + \boldsymbol{E}^{\text{in}}) = 0$ and we can rewrite (16) as

$$K^{+}_{B,1} = -\tfrac{1}{4}\iint_{B_C} \boldsymbol{E}^{\text{in}} \cdot \boldsymbol{J}^{(1)}_B \, dS = -\tfrac{1}{4}\iint_{B_C} \boldsymbol{E}^{\text{in}}_t \cdot \boldsymbol{J}^{(1)}_B \, dS. \tag{17}$$

This expression allows us to calculate by what amount the eigenmode in the interconnection $B_{I,1}$ is excited due to interaction of the incident field with the component part B_C. It is noted that only the xy-components of $\boldsymbol{E}^{\text{in}}$ come in between for the considered planar structures. As mentioned earlier we had to assume that the nonmodal part of the scattered field at the port planes $S_{B,1}$ and $S_{B,2}$ was negligible. This assumption however can be dropped as is shown in Appendix B. It is shown that if the port planes are taken further down the interconnection lines the excited modes in those lines have two different origins. The first contribution is given by (17) and the second contribution comes from the interaction of the incident field with the modal currents of the interconnection lines. This last contribution corresponds with the situation of Fig. 2. In fact, Appendix B proves that it is allowed to separate the interaction with the component part from the interaction with the interconnection lines. Let us return to the situation of Fig. 1 and assume that our incident field is the field generated by A_C. In the previous derivation it is then assumed that the structure A is located outside the surface Σ. At the same time the scattered field has to be negligible at this surface. These two assumptions will be compatible if the effect of the presence of circuit B is negligible on the working of circuit A when circuit B is not excited at his interconnections.

As a last step we have to translate the excitation coefficient $K^{+}_{B,i}$ to the sources $V_{B,1}$ and $I_{B,1}$. Using the transmission line

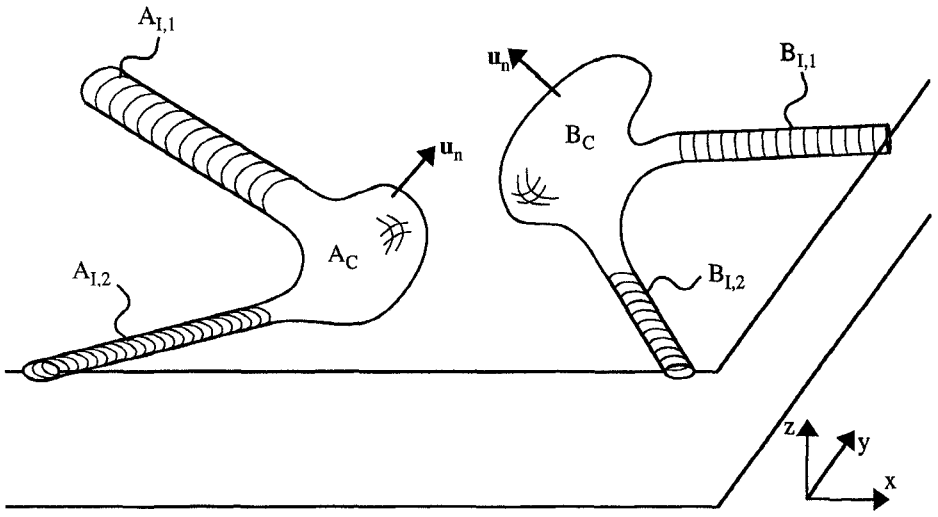

Fig. 6. Two interacting structures with arbitrarily shaped 3-D component parts and arbitrarily shaped 2-D interconnection parts embedded in a layered medium.

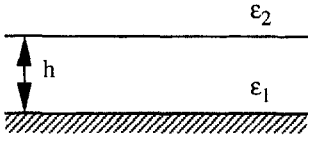

Fig. 7. Geometry of a microstrip substrate.

equivalent defined in [2] it is easy to show that these sources are given by

$$V_{B,1} = 2(I_{m,B,1})^{-1} K^{+}_{B,1}$$
$$I_{B,1} = I_{m,B,1} K^{+}_{B,1}. \tag{18}$$

These two sources generate a mode in the transmission line $B_{I,1}$ with excitation coefficient $K^{+}_{B,1}$ propagating away from B_C. If the 'b'-field in the Lorentz reciprocity theorem is the field generated by a normalized mode incident on B_C along $B_{I,2}$ then we can determine $V_{B,2}$ and $I_{B,2}$.

V. General Three-Dimensional Structures

Up to now we concentrated on planar perfectly conducting metalization structures. In this section we will generalize the previous results to general three-dimensional (3-D), not necessary perfectly conducting, objects embedded in layered media. This allows the incorporation of finite conductivity and finite thickness which is important for MCM's. In this way it is in principle possible to apply the theory also to dielectric waveguide circuits.

Consider the structure of Fig. 6 which is a 3-D generalization of the structure on Fig. 1. The interconnections $A_{I,1}, A_{I,2}, B_{I,1}$ and $B_{I,2}$ are now general open waveguides, which have been studied in for example [7], [8]. The component parts A_C and B_C are arbitrarily shaped 3-D structures connecting the interconnections. The same assumptions are made concerning the modal character of the interconnections as in the planar case. Remark that $A_{I,1}, A_{I,2}, A_C, B_{I,1}, B_{I,2}$, and B_C indicate the external surface of the structures A and B.

First, we concentrate again on the transmitter problem. The transmission line description remains the same as in the planar case, i.e., (1)–(3) remain valid [1]. Let $\boldsymbol{E}^{(i)}_A$ and $\boldsymbol{H}^{(i)}_A$ denote the electric and magnetic fields in the component part of the structure A when it is excited by a normalized mode along $A_{I,i}$. In fact we only need the equivalent electric and magnetic current densities $\boldsymbol{J}^{(i)}_A = \boldsymbol{u} \times \boldsymbol{H}^{(i)}_A$ and $\boldsymbol{K}^{(i)}_A = \boldsymbol{E}^{(i)}_A \times \boldsymbol{u}_n$ on the surface A_C. These have to follow from an electromagnetic analysis of the structure A. To determine the fields generated by $\boldsymbol{J}^{(i)}_A$ and $\boldsymbol{K}^{(i)}_A$ we have to generalize (5) to a coupled field mixed-potential formalism [9], [10]

$$\boldsymbol{E}^{(i)}(\boldsymbol{r}) = \iint_{A_C} \left\{ [\boldsymbol{G}_A(\boldsymbol{r}|\boldsymbol{r}') - \nabla\nabla G_\phi(\boldsymbol{r}|\boldsymbol{r}')] \cdot \boldsymbol{J}^{(i)}_A(\boldsymbol{r}') - \frac{1}{j\omega\epsilon} [\nabla \times \boldsymbol{G}_F(\boldsymbol{r}|\boldsymbol{r}')] \cdot \boldsymbol{K}^{(i)}_A(\boldsymbol{r}') \right\} dS'$$
$$\boldsymbol{H}^{(i)}(\boldsymbol{r}) = \iint_{A_C} \left\{ [\boldsymbol{G}_F(\boldsymbol{r}|\boldsymbol{r}') - \nabla\nabla G_\psi(\boldsymbol{r}|\boldsymbol{r}')] \cdot \boldsymbol{K}^{(i)}_A(\boldsymbol{r}') - \frac{1}{j\omega\mu} [\nabla \times \boldsymbol{G}_A(\boldsymbol{r}|\boldsymbol{r}')] \cdot \boldsymbol{J}^{(i)}_A(\boldsymbol{r}') \right\} dS' \tag{19}$$

with

$$\boldsymbol{G}_A = G_{A,tt}\boldsymbol{I}_{tt} + \nabla_t G_{A,tz}\boldsymbol{u}_z + \boldsymbol{u}_z \nabla_t G_{A,zt} + G_{A,zz}\boldsymbol{u}_z\boldsymbol{u}_z$$
$$\boldsymbol{G}_F = G_{F,tt}\boldsymbol{I}_{tt} + \nabla_t G_{F,tz}\boldsymbol{u}_z + \boldsymbol{u}_z \nabla_t G_{F,zt} + G_{F,zz}\boldsymbol{u}_z\boldsymbol{u}_z \tag{20}$$

where $G_{A,tt}, G_{A,tz}, G_{A,zt}, G_{A,zz}, G_{F,tt}, G_{F,tz}, G_{F,zt}, G_{F,zz}$, G_ϕ, and G_ψ are scalar Green's functions for the magnetic vector potential, respectively, the electric vector potential, the electric scalar potential and the magnetic scalar potential. Again all these Green's functions only depend on ρ, z and z' and hence we can proceed as in (6)–(11). However the component part A_C is now described by two sets of surface wave radiation patterns $\boldsymbol{f}^{(i)}_\nu(\varphi)$ and $\boldsymbol{g}^{(i)}_\nu(\varphi)$

$$\boldsymbol{f}^{(i)}_\nu = \iint_{A_C} \exp(j\lambda_\nu \boldsymbol{u} \cdot \Delta\boldsymbol{r}) \boldsymbol{J}^{(i)}_A(\boldsymbol{r}')\, dS'$$
$$\boldsymbol{g}^{(i)}_\nu = \iint_{A_C} \exp(j\lambda_\nu \boldsymbol{u} \cdot \Delta\boldsymbol{r})\, \boldsymbol{K}^{(i)}_A(\boldsymbol{r}')\, dS'. \tag{21}$$

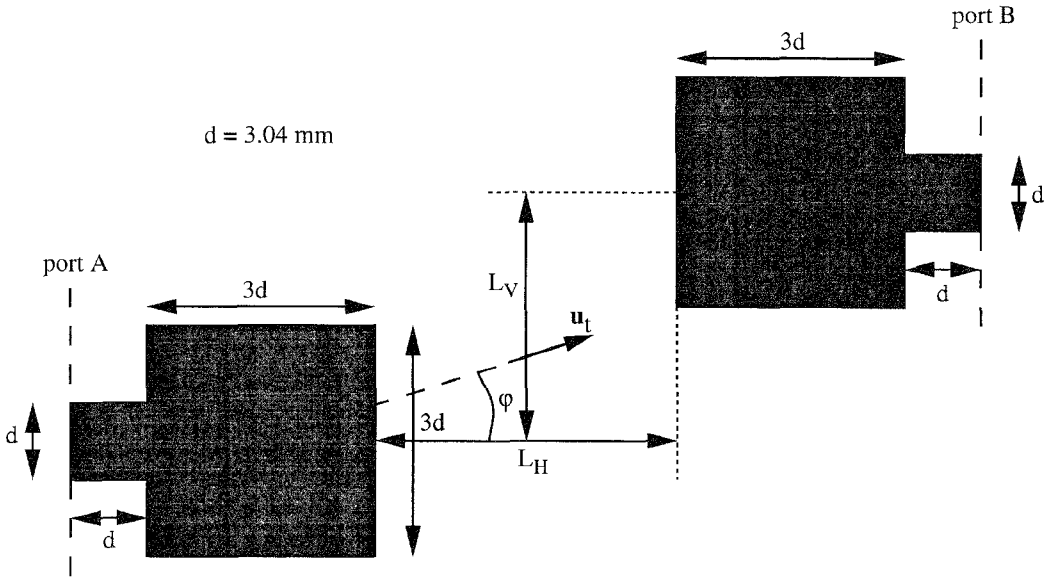

Fig. 8. Geometry of the metalization of two square patches.

Also for the observation or receiver problem we can proceed as in Section IV. By carefully applying Lorentz reciprocity theorem as is done for the 2-D case in [2] it is possible to show that (17) has to be generalized to

$$K^{+}_{B,1} = -\tfrac{1}{4} \iint_{B_C} [\boldsymbol{E}^{(1)}_B \times \boldsymbol{H}^{\text{in}} - \boldsymbol{E}^{\text{in}} \times \boldsymbol{H}^{(1)}_B] \cdot \boldsymbol{u}_n \, dS. \quad (22)$$

It has to be emphasised that $(\boldsymbol{E}^{\text{in}}, \boldsymbol{H}^{\text{in}})$ is the incident field generated by structure A in the layered medium without the presence of structure B.

VI. Application

Now we will apply the technique of Section III and Section IV to the dominant surface wave of a microstrip substrate. Fig. 7 shows the geometry of the substrate consisting of two layers above a perfectly conducting plate. The bottom layer has a thickness h and permittivity ϵ_1 and the top layer has infinite thickness and permittivity ϵ_2. Both layers are nonmagnetic, i.e., $\mu_1 = \mu_2 = \mu_0$. The spectral scalar Green's functions $G_{A,tt}(\lambda)$ and $G_\phi(\lambda)$ for $z = z' = h$ are easily determined and given by

$$\begin{aligned} G_{A,tt}(\lambda) &= \frac{Z_1'' Z_2'' \text{sh}(\Gamma_2 h)}{Z_2'' \text{sh}(\Gamma_2 h) + Z_1'' \text{ch}(\Gamma_2 h)} \\ G_\phi(\lambda) &= \frac{\text{sh}(\Gamma_2 h)}{\lambda^2} \left[\frac{Z_1' Z_2' \text{sh}(\Gamma_2 h)}{Z_2' \text{sh}(\Gamma_2 h) + Z_1' \text{ch}(\Gamma_2 h)} \right. \\ &\quad \left. + \frac{Z_1'' Z_2'' \text{sh}(\Gamma_2 h)}{Z_2'' \text{sh}(\Gamma_2 h) + Z_1'' \text{ch}(\Gamma_2 h)} \right] \end{aligned} \quad (23)$$

with

$$Z_i' = \frac{\Gamma_i}{j\omega\epsilon_i} \quad Z_i'' = -\frac{j\omega\mu_i}{\Gamma_i} \quad \Gamma_i = \sqrt{\lambda^2 - k_i^2} \quad (24)$$

with $i = 1, 2$. The propagation coefficient λ_1 of the dominant surface wave mode, which is a TM-mode, is solution of

$$Z_2' \text{sh}(\Gamma_2 h) + Z_1' \text{ch}(\Gamma_2 h) = 0 \quad (25)$$

Radiation pattern $|\mathbf{f}_1(\varphi).\mathbf{u}_t|$(Amm)

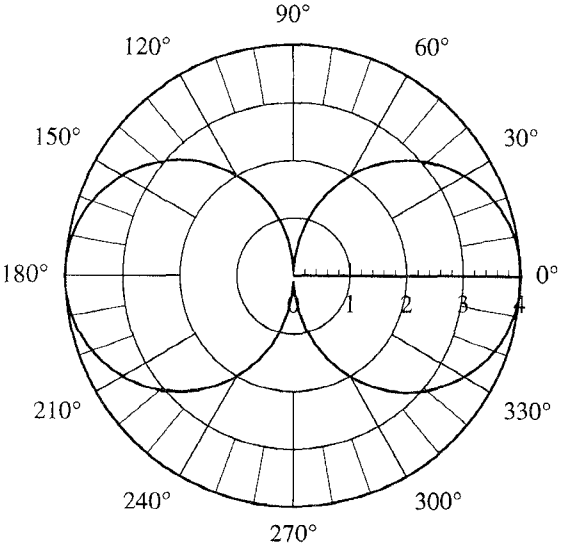

Fig. 9. Surface wave radiation pattern $|\boldsymbol{u}_t \cdot \boldsymbol{f}_1(\phi)|$ of the current distribution on the left patch of Fig. 8.

The residue $G_{\phi,1}$ of $G_\phi(\lambda)$ for this surface wave is

$$G_{\phi,1}(\lambda_1) = \frac{1}{\lambda_1^3} \frac{Z_1' Z_2'}{\dfrac{Z_2'}{\Gamma_2^2} - \dfrac{Z'^2_2 h}{Z_1' \Gamma_2} - \dfrac{Z_2'}{\Gamma_1^2} + \dfrac{Z' h}{\Gamma_2}}. \quad (26)$$

As an example we consider the configuration of Fig. 8 at a frequency of 3 GHz. The substrate has the following characteristics: $h = 3.17$ mm, $\epsilon_{r,1} = 11.7$ and $\epsilon_{r,2} = 1$. The metalization pattern consists of two square patches with dimensions 9.12 mm × 9.12 mm, separated by a horizontal distance L_H and a vertical distance L_V. Both the patches are exited by a microstrip line with width $d = 3.04$ mm. The port of each patch is taken 3.04 mm down the microstrip lines. The characteristic impedance $Z_{\text{char}} = 48.04\ \Omega$ and the propagation

coefficient $\beta = 2.9151k_0$ of the fundamental mode of the microstrip lines were calculated with a classical 2-D spectral domain moment method analysis. With a commercially available electromagnetic simulator for planar structures (HP-Momentum from HP EEsof) the current distribution on one patch was determined when excited at its port. The S_{AA}-parameter obtained by this simulator is given by $S_{AA} = 0.255 + 0.959j$. At 3 GHz the propagation coefficient of the sole surface wave above cut-off is given by $\lambda_1 = 1.022\,26k_0$ and the corresponding residue $G_{\phi,1}(\lambda_1) = 14\,075j$. Fig. 9 shows the radiation pattern $|\boldsymbol{f}_1(\phi) \cdot \boldsymbol{u}_t|$ corresponding to the current distribution of the patch. Note that for the given frequency this is almost a perfect dipole radiation pattern. Fig. 10 shows the modulus of the S_{AB}-parameter, calculated with the theory described in previous sections as a function of the horizontal distance L_H when $L_V = 0$. The dots on the figure are results obtained from an electromagnetic simulation of the total 2-port structure consisting of patch A and patch B. A good agreement is found between both results and as expected this agreement becomes even better for larger distances when the surface wave becomes more dominant. Also the phase of S_{AB} (not shown on the figure) is in good agreement. In Fig. 11 results are presented when $L_V = 0.2$ m. Fig. 12 shows an equivalent circuit for the whole structure of Fig. 8. The impedance Z is given by

$$Z = \frac{2(1 + S_{AA})}{I_m^2(1 - S_{AA})} \tag{27}$$

and the sources V_B and I_B depend on the currents i_A and are given by

$$V_B = \frac{2S_{AB}}{I_m^2(1 - S_{AA})} i_A$$
$$I_B = \frac{S_{AB}}{1 - S_{AA}} i_A \tag{28}$$

V_A and I_A follow from symmetry.

VII. Conclusion

The interaction between structures embedded in layered media was investigated. It was shown that each component can be represented by a surface wave radiation pattern. On the other hand the influence on a component of an incoming electromagnetic field was investigated by means of the Lorentz reciprocity theorem. This influence was represented by voltage and current sources at the ports of the circuit model of the component.

Appendix A

For notational simplicity we assumed in the main text that the interconnections were monomodal. In this appendix the equations are generalized to multimodal interconnections which propagate more than one mode. Important examples of multimode interconnections are coupled microstrip lines and coupled coplanar waveguides. In the circuit model these multimodal interconnections are represented by coupled transmission lines [1].

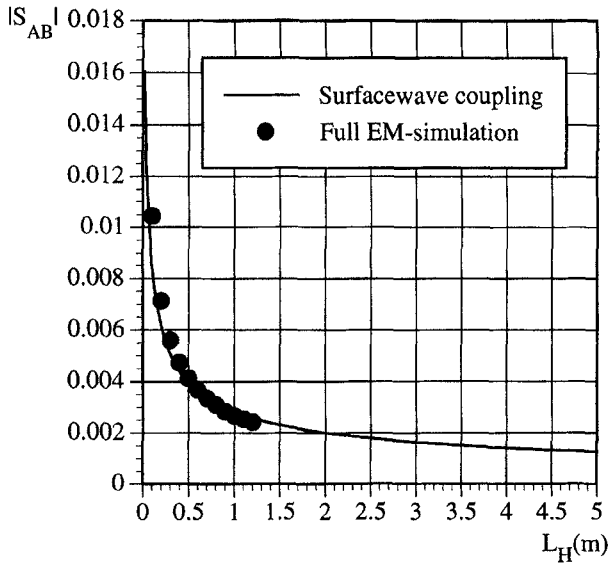

Fig. 10. $|S_{AB}|$ as a function of the horizontal distance L_H between the patches of Fig. 8 when $L_V = 0$. The full line is obtained with the theory of this paper and the dots are results from an electromagnetic simulation of the global structure.

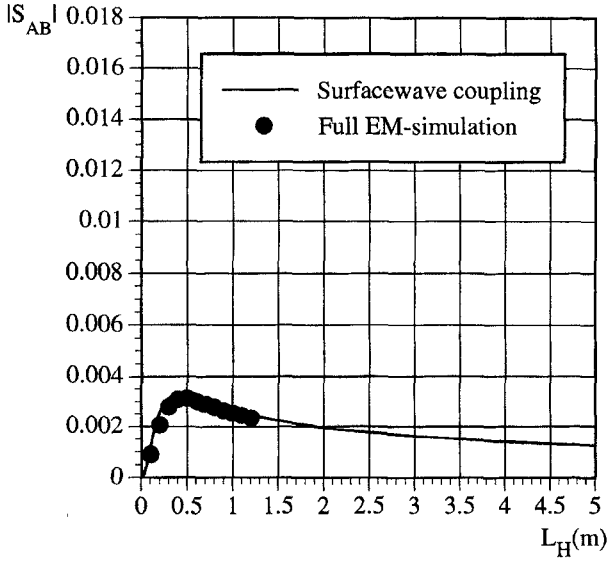

Fig. 11. $|S_{AB}|$ as a function of the horizontal distance L_H between the patches of Fig. 8 when $L_V = 0.2$ m. The full line is obtained with the theory of this paper and the dots are results from an electromagnetic simulation of the global structure.

If the interconnection $A_{I,i}$ propagates $N_{A,i}$ modes then the voltages and currents on the corresponding set of coupled transmission lines are written as

$$\underline{v}_{A,i} = 2(\underline{I}^T_{m,A,i})^{-1} \exp(-j\underline{\beta}_{A,i}s)\underline{K}^+_{A,i} + 2(\underline{I}^T_{m,A,i})^{-1} \exp(j\underline{\beta}_{A,i}s)\underline{K}^-_{A,i}$$
$$\underline{i}_{A,i} = \underline{I}_{m,A,i} \exp(-j\underline{\beta}_{A,i}s)\underline{K}^+_{A,i} - \underline{I}_{m,A,i} \exp(j\underline{\beta}_{A,i}s)\underline{K}^-_{A,i}. \tag{29}$$

This is the generalization of (1). $\underline{v}_{A,i}$ and $\underline{i}_{A,i}$ are column matrices with $N_{A,i}$ elements, $\underline{K}_{A,i}$ is a column matrix with the $N_{A,i}$ excitation coefficients of the modes, $\underline{I}_{m,A,i}$ is a

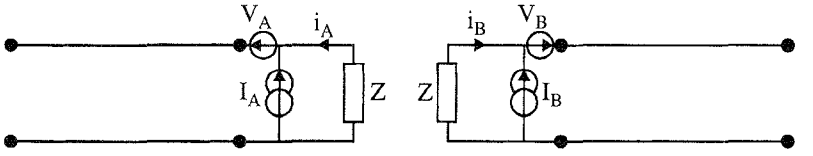

Fig. 12. Equivalent circuit for the structure of Fig. 8.

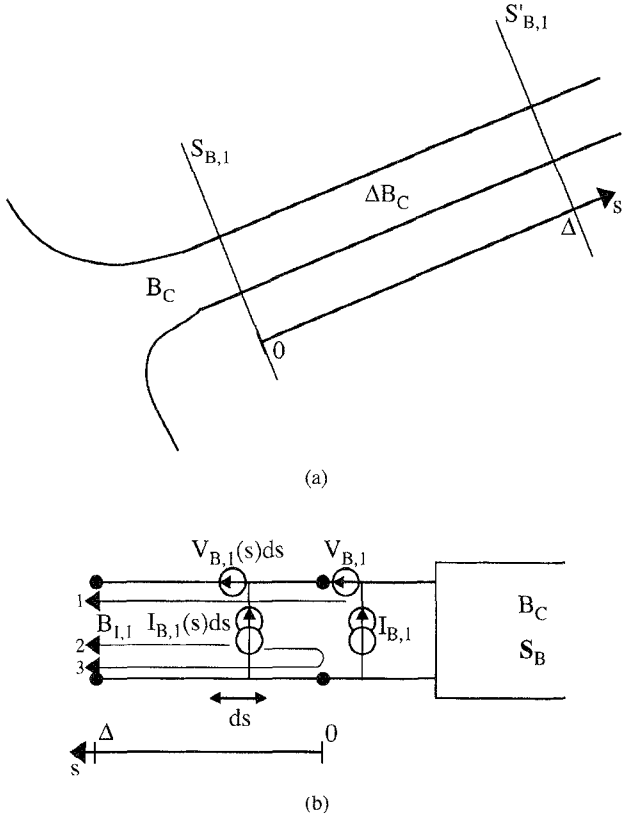

Fig. 13. Close-up of the interconnection $B_{I,1}$ to demonstrate the separability between interaction with the component part and interaction with the interconnection part.

$N_{A,\imath} \times N_{A,\imath}$ matrix with the longitudinal currents on each line for each mode [1] and $\underline{\beta}_{A,\imath}$ is a diagonal matrix with the propagation coefficients of the different modes. The inversion of (29) at $s = 0$ becomes

$$\underline{K}^{\pm}_{A,\imath} = \tfrac{1}{4}\left[\underline{I}_{m,A,\imath}\underline{v}_{A,\imath}(s=0) \pm 2(\underline{I}_{m,A,\imath})^{-1}\underline{i}_{A,\imath}(s=0)\right] \tag{30}$$

If the structure A is excited by normalized modes along for example $A_{I,1}$, then we get the following current densities on the structure A

$$\begin{aligned}
\underline{\boldsymbol{J}}^{(1)}_{A,1} &= \exp(j\underline{\beta}_{A,1}s)(-\underline{J}_{s,A,1}\boldsymbol{u}_s + \underline{J}_{\mathrm{tr},A,1}\boldsymbol{u}_{\mathrm{tr}}) \\
&\quad + \underline{S}_{A,11}\exp(-j\underline{\beta}_{A,1}s)(\underline{J}_{s,A,1}\boldsymbol{u}_s + \underline{J}_{\mathrm{tr},A,1}\boldsymbol{u}_{\mathrm{tr}}) \\
&\qquad\qquad \text{on } A_{I,1} \\
\underline{\boldsymbol{J}}^{(1)}_{A,2} &= \underline{S}_{A,12}\exp(j\underline{\beta}_{A,2}s)(\underline{J}_{s,A,2}\boldsymbol{u}_s + \underline{J}_{\mathrm{tr},A,2}\boldsymbol{u}_{\mathrm{tr}}) \quad \text{on } A_{I,2} \\
\underline{\boldsymbol{J}}^{(1)}_{A} &\qquad\qquad \text{on } A_C
\end{aligned} \tag{31}$$

where $\underline{S}_{A,11}$ is a $N_{A,\imath} \times N_{A,\imath}$ submatrix of $\boldsymbol{S}_A$, describing the reflections and cross-reflections of the $N_{A,1}$ modes at the component part A_C. The remaining part of the transmitter problem is easily generalized to multimodal interconnections. We just want to mention the generalization of (11)

$$\underline{\boldsymbol{f}}^{(\imath)}_{\nu}(\varphi) = \iint_{A_C} \exp(j\lambda_\nu \boldsymbol{u}_t \cdot \Delta\boldsymbol{r})\underline{\boldsymbol{J}}^{(\imath)}_{A}(\boldsymbol{r}')\, dS' \tag{32}$$

where $\underline{\boldsymbol{f}}^{(\imath)}_{\nu}$ is a column matrix with $N_\imath$ elements representing the surface wave radiation patterns of surface wave ν generated by each of the modes at all the interconnections.

The receiver problem equations (12)–(14) are easily generalized as in (31). Finally (17) and (18) are generalized as

$$\underline{K}^{+}_{B,1} = -\tfrac{1}{4}\iint_{B_C} \boldsymbol{E}^{\mathrm{in}}_t \cdot \boldsymbol{J}^{(1)}_B\, dS \tag{33}$$

and

$$\begin{aligned}
\underline{V}_{B,1} &= 2(\underline{I}^T_{m,B,1})^{-1}\underline{K}^{+}_{B,1} \\
\underline{I}_{B,1} &= \underline{I}_{m,B,1}\underline{K}^{+}_{B,1}.
\end{aligned} \tag{34}$$

Appendix B

In this Appendix we will show that it is allowed to separate the interaction of an externally incident field with the interconnection lines from the interaction with the component part. Let us concentrate on the close-up on Fig. 13(a) of the interconnection $B_{I,1}$ and the component part B_C. In stead of taking the port at $S_{B,1}$, i.e., $s = 0$, we now take the port further down the line at $S'_{B,1}$, i.e., $s = \Delta$. In this way the component part increases by an amount ΔB_C. The currents $\boldsymbol{J}_b$ of the 'b'-field on ΔB_C are modal and take the following form (see also (4)):

$$\begin{aligned}
\boldsymbol{J}_b = \boldsymbol{J}^{(1)}_{B,1} &= \exp(j\beta_{B,1}s)(-J_{s,B,1}\boldsymbol{u}_s + J_{\mathrm{tr},B,1}\boldsymbol{u}_{\mathrm{tr}}) \\
&\quad + S_{B,11}\exp(-j\beta_{B,1}s)(J_{s,B,1}\boldsymbol{u}_s + J_{\mathrm{tr},B,1}\boldsymbol{u}_{\mathrm{tr}}) \\
&\quad \text{on } \Delta B_C.
\end{aligned} \tag{35}$$

If we now proceed as in (17) we get the following result for the excitation coefficient $K'^{+}_{B,1}$ at the port plane $S'_{B,1}$

$$\begin{aligned}
K'^{+}_{B,1} = &-\tfrac{1}{4}\iint_{B_C} \boldsymbol{E}^{\mathrm{in}}_t \cdot \boldsymbol{J}^{(1)}_B\, dS - \tfrac{1}{4}\iint_{\Delta B_C} \boldsymbol{E}^{\mathrm{in}}_t \\
&\cdot [\exp(j\beta_{B,1}s)(-J_{s,B,1}\boldsymbol{u}_s + J_{\mathrm{tr},B,1}\boldsymbol{u}_{tr})]\, dS \\
&- \tfrac{1}{4}S_{B,11}\iint_{\Delta B_C} \boldsymbol{E}^{\mathrm{in}}_t \\
&\cdot [\exp(-j\beta_{B,1}s)(J_{s,B,1}\boldsymbol{u}_s + J_{\mathrm{tr},B,1}\boldsymbol{u}_{\mathrm{tr}})]\, dS
\end{aligned} \tag{36}$$

We can rewrite this as

$$K^{+}_{B,1} = K'^{+}_{B,1} + \int_0^{\Delta} K^{+}_{B,1}(s)\exp(j\beta_{B,1}s)\,ds + S_{B,11}\int_0^{\Delta} K^{-}_{B,1}(s)\exp(-j\beta_{B,1}s)\,ds \quad (37)$$

where we used (17) for the first term on the right-hand side of (36). In the two other terms on the right-hand side we separated the longitudinal integration in the s-direction from the transverse integration. The transverse integration is incorporated in the definition of the distributed excitation coefficients $K^{+}_{B,1}(s)\,ds$ and $K^{-}_{B,1}(s)\,ds$

$$K^{+}_{B,1}(s)\,ds = \tfrac{1}{4}\int_c \boldsymbol{E}^{\text{in}}_t \cdot (-J_{s,B,1}\boldsymbol{u}_s + J_{s,B,\text{tr}}\boldsymbol{u}_{\text{tr}})\,dc\,ds$$
$$K^{-}_{B,1}(s)\,ds = \tfrac{1}{4}\int_c \boldsymbol{E}^{\text{in}}_t \cdot (\boldsymbol{J}_{s,B,1}\boldsymbol{u}_s + J_{s,B,\text{tr}}\boldsymbol{u}_{\text{tr}})\,dc\,ds \quad (38)$$

where c is a transversal integration line on ΔB_C. The last two terms in (37) are represented in the circuit-model as distributed sources $V_{B,1}(s)\,ds$ and $I_{B,1}(s)\,ds$ in the transmission line $B_{I,1}$ with the theory of [2]. Remark that the longitudinal integrals of the excitation coefficients $K^{+}_{B,1}(s)\,ds$ and $K^{-}_{B,1}(s)\,ds$ with the phase factors $\exp(j\beta_{B,1}s)$ and $\exp(-j\beta_{B,1}s)$ correspond to the coefficients P and Q defined in [2]. The first term on the other hand is represented by the discrete sources $V_{B,1}$ and $I_{B,1}$ given in (18). Hence, the excitation coefficient $K'^{+}_{B,1}$ can be interpreted to consists of three parts indicated by the arrows on Fig. 13b. The first part is directly generated by the discrete source at $s = 0$ or in other words by the interaction of the incident field with the component part B_C. The second and third part are generated by the distributed sources or in other words by interaction of the incident field with the interconnection line. The second part is a direct wave and the third part an indirect wave which partly reflects at the component part, i.e., at $s = 0$.

ACKNOWLEDGMENT

The author would like to thank N. Faché and his team at HP EEsof—Alphabit in Belgium and D. De Zutter for carefully reading the manuscript and for his useful suggestions.

REFERENCES

[1] F. Olyslager, D. De Zutter, and A. T. de Hoop, "New reciprocal circuit model for lossy waveguide structures based on the orthogonality of the eigenmodes," *IEEE Microwave Theory Tech.*, vol. 42, no. 12, pp. 2261–2269, Dec. 1994.

[2] D. De Zutter and F. Olyslager, "High-frequency reciprocity based circuit model for the incidence of electromagnetic waves on general waveguide structures," *IEEE Microwave Theory Tech.*, vol. 43, no. 8, pp. 1826–1833, Aug. 1995.

[3] R. F. Harrington, *Field Computations by Moment Methods.* New York: Macmillan, 1968.

[4] L. B. Felsen and N. Marcuvitz, *Radiation and Scattering of Waves.* Englewood Cliffs, NJ: Prentice-Hall, 1973.

[5] S. Barkeshli and P. H. Pathak, "Radial propagation and steepest descent path integral representations of the planar microstrip dyadic Green's function," *Radio Science,* vol. 25, no. 2, pp. 161–174, Mar.–Apr. 1990.

[6] M. Abramowitz and I. A. Stegun, Eds., *Handbook of Mathematical Functions with Formulas, Graphs and Mathematical Tables.* New York: Dover, 1970.

[7] F. Olyslager, D. De Zutter, and K. Blomme, "Rigorous analysis of the propagation characteristics of general lossless and lossy multiconductor transmission lines in multilayered media," *IEEE Trans. Microwave Theory Tech.*, vol. 41, no. 1, pp. 79–88, Jan. 1993.

[8] F. Olyslager and D. De Zutter, "Rigorous boundary integral equation solution for general isotropic and uniaxial anisotropic dielectric waveguides in multilayered media including, losses, gain and leakage," *IEEE Trans. Microwave Theory Tech.*, vol. 41, no. 8, pp. 1385–1392, Aug. 1993.

[9] J. R. Mautz and R. F. Harrington, "Electromagnetic scattering from a homogeneous material body of revolution," *Arch. Elek. Übertragung,* vol. 33, no. 4, pp. 71–80, Apr. 1979.

[10] K. Umashankar, A. Taflove, and S. M. Rao, "Electromagnetic scattering by arbitrary shaped three-dimensional homogeneous lossy dielectric objects," *IEEE Trans. Antennas Propagat.*, vol. 34, no. 6, pp. 758–766, June 1986.

Frank Olyslager (S'90–M'94) was born in Wilrijk, Belgium, on November 24, 1966. He finished high school in 1984 and received the electrical engineering degree from the University of Ghent, Belgium, in July 1989. In 1993, he received the Ph.D. degree from the Laboratory of Electromagnetism and Acoustics (LEA) of the University of Ghent with a thesis entitled: Electromagnetic Modeling of Electric and Dielectric Waveguides in Layered Media.

At present he is a Postdoctoral Researcher of the National Fund for Scientific Research of Belgium in the Department of Information Technology (the former LEA) of the University of Ghent. From 1989 until 1993 he was a Research Assistant of the National Fund for Scientific Research of Belgium. His research deals with the use of integral equation techniques to numerically solve Maxwell's equations. His activities focus on the electromagnetic wave propagation along high frequency electrical and optical interconnections in multilayered isotropic and bianisotropic media, on the singularity of electromagnetic fields at edges and tips, and on the study of Green's dyadics in bianisotropic media. He is also investigating the construction of transmission line models for general waveguide structures and different aspects of electromagnetic compatibility (EMC) problems on printed circuit boards and microwave circuits. He spent several scientific visits at the Electromagnetics Laboratory at the Helsinki University of Technology. He is author or co-author of about 35 papers in international journals and about 25 papers in conference proceedings. He is also co-author of the book *Electromagnetic and Circuit Modeling of Multiconductor Lines* (Clarendon Press, 1993) in the Oxford Engineering Science Series.

In 1994, Dr. Olyslager became laureate of the Royal Academy of Sciences, Literature, and Fine Arts of Belgium. In May 1995 he received The IEEE Microwave Prize. Currently he is Associate Editor of *Radio Science.*